Late Mesozoic Volcanism in the Ust'-Kara Basin (Eastern Transbaikalia) and Its Relationship with Magmatism of the Great Xing'an and East Mongolian Volcanic Belts

F.M. Stupak✉, V.V. Yarmolyuk, E.A. Kudryashova

Institute of Geology of Ore Deposits, Petrography, Mineralogy and Geochemistry, Russian Academy of Science,
Staromonetnyi per. 35, Moscow, 119017, Russia

Abstract—The origin of the Late Jurassic–Early Cretaceous volcanism within the northern part of the Argun terrane (eastern Transbaikalia) is considered. New data on the geology, age, and composition of late Mesozoic volcanic complexes of the Ust'-Kara basin are presented. Three stages of volcanism have been identified: Tithonian–Berriasian (~150–143 Ma), Valanginian (~140–136 Ma), and Hauterivian (~134–131 Ma), during which volcanic rocks and sediments of three formations (Udyugan, Ust'-Kara, and Shilka, respectively) were deposited. The petrochemical and geochemical characteristics of the rocks of these formations are considered. The compositions of chemically similar rocks evolved toward an increase in the contents of incompatible elements. The rocks of the Ust'-Kara basin are compared with the coeval igneous rocks of the Great Xing'an and East Mongolian belts, which formed in the settings of an active margin and intracontinental rifting, respectively. It is shown that the rocks of the basin are similar in composition to the volcanics of the Great Xing'an belt. A conclusion has been drawn that the late Mesozoic magmatism in the northern part of the Argun terrane was controlled by subduction processes, which led to the formation of the late Mesozoic active continental margin of the Asian continent.

Keywords: Late Mesozoic volcanism, geochemical correlations, eastern Transbaikalia, Great Xing'an belt, East Mongolian belt

INTRODUCTION

In the late Mesozoic, a large volcanic province, ~4 mln km^2 in area, appeared in East Asia. Its eastern margin ran along the border of the Asian continent, and most of the province extended deep in the continent (~1200 km). The province comprises several synchronously formed volcanic areas: Gobi–Altai, East Mongolian, West Transbaikalian, Aldan, and Great Xing'an (Yarmolyuk et al., 1995). They evolved in different geodynamic settings, which determined specific magmatism in them. For example, the Great Xing'an volcanic belt formed on the continental margin, near the zone of convergence of oceanic and continental lithospheric plates, and was characterized by calc-alkalic magmatism typical of such zones (Zhang et al., 2008b). The other volcanic areas were related to intraplate rifting, which gave rise predominantly to basic magmatism in them (Yarmolyuk et al., 1995). The spatial isolation of these volcanic areas and the difference in the composition of their igneous rock associations and in their structural position do not hamper determining the boundaries between the zones of convergent and intraplate processes within the province. An

exception is the Argun terrane lying at the intersection of the extensions of the Great Xing'an and East Mongolian belts (Fig. 1). The boundary between volcanic areas of different geodynamic settings here is still unclear, as well as the mechanisms of magma formation that exerted the main influence on the composition of magmatic products in the terrane. To solve this problem, we studied volcanism in the Ust'-Kara basin located at the intersection of the above volcanic belts in the northern part of the Argun terrane, near the Mongolo-Okhotsk suture (Fig. 1).

Before the description of the late Mesozoic magmatism in the Ust'-Kara basin, we will briefly consider the major characteristics of magmatism of different types in the above two volcanic belts, which mark its different sources.

The Great Xing'an (GX) volcanic belt originated in the Middle–Late Jurassic (~166–145 Ma (Xu et al., 2013)). It is a period when the volcanic complexes of the Shadoron basin formed within the Argun terrane (Stupak et al., 2016). They were traced along the boundaries between the Argun terrane and the structures of the Aga plate and then to the south, to the territory of China, where the corresponding Tamulangou Formation of trachyandesites and basaltic trachyandesites is located (Xu et al., 2013). The Shadoron Group includes andesites, dacites, latites, and quartz latites as well as their lava breccias and tuffs with low contents of TiO_2 and total Fe_2O_3 and high contents of Al_2O_3 and MgO. The group is coeval

---

✉Corresponding author.

E-mail adress: fms38@mail.ru (F.M. Stupak)
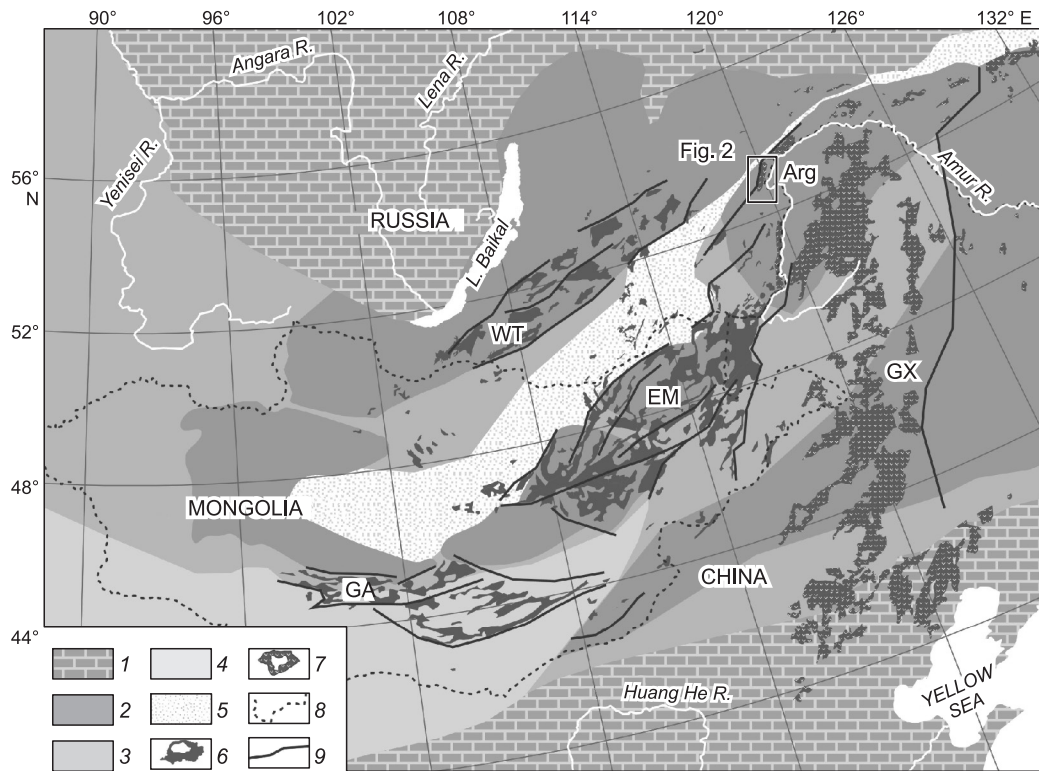
Fig. 1. Schematic structure of the late Mesozoic magmatic province of Central and East Asia (Daukeev et al., 2008). *1*, cratons; *2–5*, folded areas: *2*, late Neoproterozoic (Arg, Argun terrane), *3*, early Paleozoic (early Caledonian), *4*, middle–late Paleozoic (Hercynian), *5*, Mongolo–Okhotsk; *6–7*, lava fields: *6*, rift areas (WT, West Transbaikalian; EM, East Mongolian; GA, Gobi–Altai), *7*, Great Xing'an (GX) belt; *8*, state borders; *9*, faults. Rectangle shows the location of the Ust'-Kara basin.

with the monzonitic granitoids of the Shakhtama complex formed within ~162–155 Ma (Berzina et al., 2013). The later stages of the evolution of the GX belt were studied in its Chinese part, where the Jixiangfeng and Manitu Formations composed of rhyolites, their tuffs, and mafic rocks (~145–138 Ma) and the Yiliekede Formation made up of basalts and basaltic andesites (125 ± 10 Ma) are located (Wang et al., 2006; Zhang et al., 2008b; Xu et al., 2013). The most mafic rocks of these associations are characterized by low contents of TiO_2 (<1.5 wt.%) and a negative Ta–Nb anomaly on their spidergrams. The geologic position of the volcanic belt, confined to the edge of the paleocontinent, and the geochemical characteristics typical of convergent settings indicate that the magmatism of the belt took place on the active continental margin (Zhang et al., 2008b; Xu et al., 2013).

The East Mongolian (EM) volcanic belt covers a large part of Eastern Mongolia and the Argun area of Russia. Available geological and geochronological data (Dash et al., 2015; Stupak et al., 2018a) show a prevalence of early Early Cretaceous (~130–120 Ma) volcanic strata within the belt. These are lava strata composed of trachybasalts and basaltic trachyandesites, which form systems of wide basins and grabens of NE strike. Some trachyte-trachyrhyolite volcanoes and extrusions are dated at the middle Early Cretaceous. The

volcanic strata formed in the second half of the Early Cretaceous (~120–100 Ma) are composed mostly of trachybasalts and basaltic trachyandesites. They form predominantly separate lava fields. Late Cretaceous volcanics have an alkaline composition (tephrites and teshenites) and form systems of domes, stocks, and laccoliths. In general, the mafic rocks of the EM volcanic belt are characterized by high contents of TiO_2 (>2 wt.%) and most of incompatible elements, including Ta and Nb (Pavlova et al., 1990; Shatkov et al., 2010; Dash et al., 2015; Stupak et al., 2018a). In these characteristics of magmatism the EM belt is similar to other late Mesozoic rift areas of Central Asia which formed with the participation of mantle plumes (Yarmolyuk et al., 1995).

Thus, the above belts differ both in geologic position and in the type of magmatism. The latter difference is particularly serious and thus can be used to establish the geologic position of the Ust'-Kara basin.

GEOLOGY OF THE UST'-KARA BASIN

The Ust'-Kara basin is located in southeastern Transbaikalia, in the middle reaches of the Shilka River, stretching as a narrow band for ~40 km along both of its shores between the Shilkinskii Zavod and Nizhnie Kularki Villages (Fig. 2).
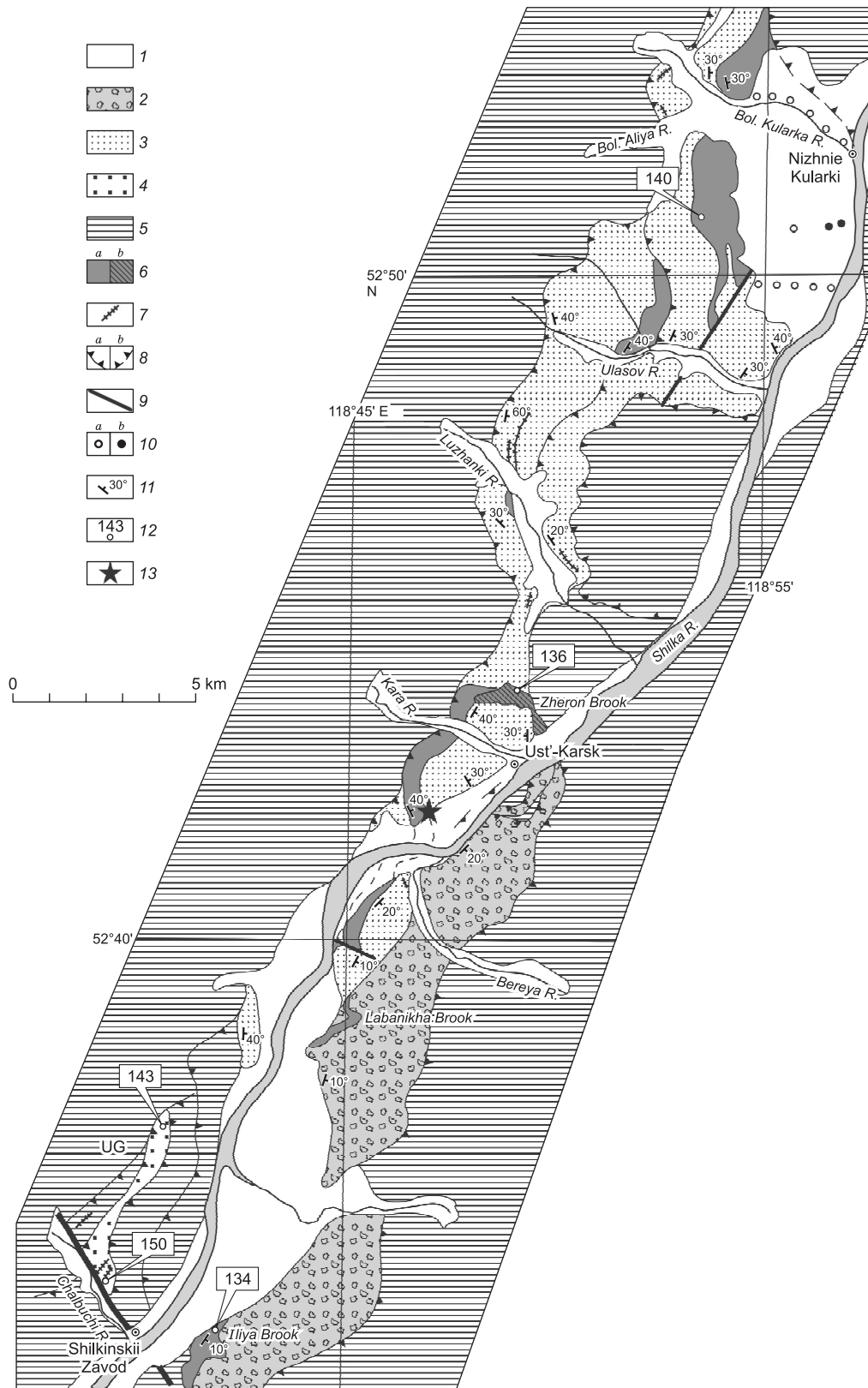
Fig. 2. Geologic structure of the Ust'-Kara basin. *1*, Quaternary deposits; *2–4*, Late Jurassic–Early Cretaceous sedimentary and volcanic rocks of formations: *2*, Shilka, *3*, Ust'-Kara, *4*, Urdyugan; *5*, rocks of the pre-Cretaceous basement; *6*, Early Cretaceous lavas (*a*) and intrusions (*b*); *7*, thin flows and dikes; *8*, thrusts and shifts: observed (*a*), overlapped (*b*); *9*, normal faults; *10*, boreholes with sedimentary (*a*) and volcanic (*b*) rocks in the faces; *11*, direction and angle of dip of rock beds; *12*, localities of sampling of rocks and their age (Ma); *13*, exposure of rhyolite tuffs of the Ust'-Kara Formation.

Two grabens are recognized within the basin: Ust'-Kara and Urdyugan. There is an opinion (Misnik and Shevchuk, 1975), which we support, that this basin is a relic of a larger negative structure, the Boty–Kara basin, extending southward to the Boty Village, where one more large relic of this structure, the Kuma River graben, occurs (Stupak, 2012).

The Ust'-Kara basin is superposed on the structures of different ages of the Argun terrane, which are composed of complexes of igneous, sedimentary, and metamorphic rocks formed in the Late Riphean–Late Jurassic (State..., 2010). The basin is located in the Argun terrane zone confined to the area of the expected intersection of the structures of the EM and GX belts. Therefore, it has a key importance for understanding which of the belts exerted the major effect in this part of the late Mesozoic magmatic province.

The Ust'-Kara basin is a bilateral graben. Along its eastern border, the structures of the pre-Cretaceous basement are thrust over the volcanic and sedimentary rocks of the graben at an angle of ~30°. Its western border is a strike-slip fault of steeper dip opposite to the direction of the thrust.

In the southern part of the graben, on the left bank of the Shilka River, one of the branches of this strike-slip fault controls a separate small (~1 × 7 km) **Urdyugan graben** (Fig. 2). It is filled mostly with coarse-clastic red-colored deposits and volcanics of the Urdyugan Formation, which are the oldest of the late Mesozoic rocks of the Ust'-Kara basin. The volcanics are mainly of subvolcanic facies. Among them, there are dikes and stocks of basaltic-andesite and andesite porphyry in the south of the graben and extrusions of quartz–biotite porphyry in the north. The section of the Urdyugan Formation is rich in sedimentary rocks with varying amounts of volcanic material (tuffs, tuffites, tuff conglomerates, and tuffstones). The total thickness of the visible part of the section varies from 360 to 500 m. The K–Ar dating of the volcanics of this formation yields its late Late Jurassic–Early Cretaceous age (Table 1).

The Ust'-Kara graben and the Kuma River graben are formed by younger Early Cretaceous terrigenous-sedi-mentary and igneous rocks. Since the research by Voinovskii-Kriger and Lisovskii (1927), their strata have been divided into two formations, Ust'-Kara (lower) and Shilka (upper). Figure 2 shows that the rocks of the Ust'-Kara Formation occur in the northern part of the graben, along the left bank of the Shilka River, and the rocks of the Shilka Formation occupy the right bank of the river, from the Ust'-Karsk Village to the southernmost border of the graben. The rocks of the Ust'-Kara Formation penetrate to the right bank of the Shilka River only at a short segment between the mouths of the Bereya River and the Labanikha Brook, where they tectonically join the deposits of the Shilka Formation.

The Ust'-Kara Formation is composed of terrigenous and volcanic rocks. The terrigenous deposits are predominant rocks of the series fine-pebble conglomerate–siltstone and subordinate coarse psephites (Pistsov, 1982). Volcanic rocks occur in the middle section of the formation. They are recognized as a subformation extending over the area of the Ust'-Kara deposits. Its thickness reaches 350 m in the north of the graben (Ulasov–Bol'shaya Kularka interfluve) and decreases to 250 m in the south. Terrestrial trachyandesite–trachyte lavas are replaced by subaquatic pillow lavas and basaltic-trachyandesite hyaloclastites to the south from the Luzhanki River. Also, dikes and stocks of these rocks appear here, and the number of sedimentary beds increases. The upper section of the formation is made up of rhyolitic tuffs.

A specific tectonic feature of the Ust'-Kara Formation is its almost ubiquitous monoclinic occurrence with the eastward dip of rock beds and with thrusts: a thrust of the formation beds over each other in the Ulasov–Luzhanki interfluve and a thrust of a plate of lower Cambrian brecciated carbonate rocks over the formation rocks. The total thickness of the formation rocks is 1300 m (Pistsov, 1963). The estimated age of the Ust'-Kara Formation is debatable: Based on the found paleontological relics, the formation is dated at the Late Jurassic–Early Cretaceous (Pistsov, 1963; Misnik and Shevchuk, 1975) or at the Late Jurassic (Geologic..., 1997;

Table 1. Results of geochronological studies of rocks of the Ust'-Kara basin

Formation (association)	Sample	Rock	Sampling locality	K–Ar		Age, Ma ($\pm 2\sigma$)
				Potassium, % ($\pm \sigma$)	^{40}Ar, ppb ($\pm \sigma$)	
Shilka	99-3*	Anamesitic trachyandesite	Kuma River	2.32 ± 0.03	21.95 ± 0.10	131.5 ± 3
	99-29		Iliya Brook	1.98 ± 0.02	19.14 ± 0.09	134 ± 3
Ust'-Kara	22-97	Trachyandesite	Zheron Brook	2.70 ± 0.03	26.36 ± 0.10	136 ± 3
	3-97**	Trachyandesite	Ulasov–Bol'shaya Aliya interfluve	$^{40}Ar/^{39}Ar$ Plateau age—139.7 ± 1.3; Integrated age—140.0 ± 1.6		
Urdyugan	99-22	Quartz–biotite rhyolite	Urdyugan River, left bank	4.35 ± 0.04	44.95 ± 0.16	143 ± 3
	99-16	Two-pyroxene andesite	Chalbuchi River, left bank	2.14 ± 0.03	23.28 ± 0.08	150 ± 4

Note. The bulk rock was analyzed. For K–Ar dating, the contents of ^{40}Ar were measured by the isotope dilution method, using ^{38}Ar as a tracer, and the contents of K, by flame photometry. The age was calculated using constants (Steiger and Jager, 1977) $\lambda_K = 0.581 \times 10^{-10}$ yr^{-1}, $\lambda_{\beta-} = 4.962 \times 10^{-10}$ yr^{-1}, and $^{40}K = = 0.01167$ (at.%). 99-3*, data by Stupak (2012); 3-97**, $^{40}Ar/^{39}Ar$ data by Stupak and Travin (2004).

State..., 2010). Our geochronological data (Table 1) show an Early Cretaceous age.

The coarse-clastic deposits of the Shilka Formation lie, with erosion, over the Ust'-Kara deposits. The lower section of the formation is made up of less coarse clastics (boulder–pebble and pebble conglomerates), which give way to ubiquitous fanglomerates upsection (Pistsov, 1982). In the Ust'-Kara graben, there are local flows and sills of trachyandesites and basaltic trachyandesites (Fig. 2). The thickness of their members reaches 100 m in the area of the Labanikha Brook and 150 m in the Iliya Brook on the southern border of the graben, where the maximum thickness (up to 800 m) of the formation rocks is also observed.

The Early Cretaceous volcanism and sedimentation were still more intense on the southwestern border of the Boty–Kara basin. Here, a 4350 m thick unit of mostly coarse terrigenous sediments and volcanics exposes in the relict graben along the Kuma River (Stupak, 2012). These deposits are similar to the deposits of the Shilka Formation of the Ust'-Kara graben; their beds are monoclinically subsided eastward, which indicates that the two structures were a single whole in the past. A distinctive feature of the Kuma graben volcanics is the wide occurrence of their subaquatic varieties (hyaloclastites and pillow and nucleus lavas). Four flows of terrestrial lavas are found only in the lower section. Dating of one of them yielded an Early Cretaceous age of lavas (Table 1). The Kuma graben also has felsic rocks. A small (100 × 50 m) quartz porphyry stock breaks through the lower bed of a terrigenous rock unit in the northern part of the graben. Porphyry underwent intense hydrothermal alteration (silicification and argillization).

ANALYTICAL METHODS

The age of volcanics was determined by K–Ar dating in the Laboratory of Isotope Geochemistry and Geochronology of the Institute of Geology of Ore Deposits, Petrography, Mineralogy, and Geochemistry, Moscow, following the technique described by Lebedev et al. (1999) and Chernyshev et al. (2006). For analysis, a fine-grained rock groundmass cleaned from rock-forming phenocrysts was used.

The contents of major rock elements were measured by the X-ray fluorescence method (XRF) on an PW 2400 Philips Analytical spectrometer at the Institute of Geology of Ore Deposits, Petrography, Mineralogy, and Geochemistry, Moscow.

Multielement analysis of rocks was carried out on a PlasmaQuad 3 VG Elemental mass spectrometer with inductively coupled plasma at the Institute for Analytical Instrumentation, St. Petersburg. To control the drift of the relative sensitivity of the mass spectrometer, analysis of several samples (no more than 5–10) was made together with analysis of standard solutions of heavy metals (Ti, Cr, Ni, Cu, and Pb) and the standard sample BCR-1. For REE analysis, the mass spectrometer was calibrated against a Matthew Johnson standard REE solution. The relative error of analyses was within 5–10%.

RESULTS OF GEOCHRONOLOGICAL STUDY

As noted above, paleontological dates of the graben rocks are ambiguous. Geochronological study of volcanics of the three graben formations (Table 1) showed a systematic difference in their ages, which agrees with the data of geological study. For example, the age of andesitic porphyrites (150 ± 4 Ma) and quartz–biotite porphyry (143 ± 3 Ma) of the Urdyugan Formation confirmed their earliest origin. Trachyandesite lavas (140 ± 1.6 Ma) of the Ust'-Kara Formation and trachyandesite sill (136 ± 3 Ma) are younger. They are close in age to the trachyandesite lavas of the Ust'-Kara (134 ± 3) and Kuma (131.5 ± 1.6 Ma (Stupak, 2012) grabens. In general, the established ages correspond to the time of accumulation of the Jixiangfeng, Manitu (~150–138 Ma), and Yiliekede (~135–120 Ma) Formations of the GX belt (Wang et al., 2006; Zhang et al., 2008b; Xu et al., 2013), composed both of felsic and mafic volcanics. Within the EM volcanic belt, volcanism of this age range is of limited manifestation.

PETROGRAPHY

The volcanics of the Urdyugan Formation are basaltic andesites, andesitic porphyrites, and quartz–biotite porphyry. In rocks of normal composition, phenocrysts amount to 15–20 vol.%, with orthopyroxene significantly dominating over clinopyroxene. The phenocrysts are localized in the pilotaxitic groundmass composed of finest plagioclase laths, magnetite grains, and totally devitrified volcanic glass. The felsic volcanics contain up to 40 vol.% phenocrysts (with prevailing K–Na-feldspar), up to 10 vol.% biotite, and single quartz grains localized in the fine-grained quartz–feldspar groundmass.

The volcanics of the Ust'-Kara Formation are mostly of the trachyandesite–trachyte series. They are usually porphyritic and contain a small amount (1–5%) of fine phenocrysts of predominant plagioclase (from oligoclase to felsic andesine), subordinate clinopyroxene and amphibole, and K–Na-feldspar (in more felsic varieties). Their minerals are localized in the pilotaxitic groundmass composed mainly of plagioclase, magnetite, and volcanic glass significantly replaced by secondary minerals. In hyaloclastites, the glass is greenish, partly replaced by palagonite–chlorophaeite.

The rhyolite tuffs of the Ust'-Kara Formation are composed of clastics of almost completely devitrified volcanic glass. They contain lamellar biotite crystals and fragments of porphyritic grains of K–Na-feldspar, whose size decreases from 1–3 mm in the bottom of the tuff bed to fractions of mm in its top.

Subvolcanic analogues of the Ust'-Kara lavas have a similar mineral composition and differ from them in finer

grains (similar to dolerite ones), the absence of amphibole (they are biotite lavas), and, often, the presence of late quartz.

The volcanics of the Shilka Formation correspond to trachyandesites and basaltic trachyandesites and contain mostly phenocrysts of felsic andesine. The large phenocrysts are usually resorbed, and the small ones form glomerocrysts, sometimes together with clinopyroxene. The rock groundmass is formed by microdiabase (anamesitic) with transitions into pilotaxite; it consists of predominant plagioclase (70–75%) and subordinate clinopyroxene, magnetite, and altered volcanic glass. Subvolcanic analogues of these rocks (sills and dikes) have the same composition and structures.

THE PETROCHEMICAL AND GEOCHEMICAL COMPOSITIONS OF ROCKS

As follows from Table 2 and Fig. 3, most of the late Mesozoic volcanics of the Ust'-Kara basin and Kuma River graben are normal or felsic medium-alkali rocks. Only a minor part of them, mainly the rocks of the Urdyugan Formation, fall in the normal-alkalinity field. In the K_2O–SiO_2 diagram (Fig. 3), most of the composition points lie in the field of high-K rocks. Almost all rocks are quartz- and hypersthene-normative. Some of them contain normative olivine, and few rocks, nepheline. Normative corundum (up to 4%) typical of these rocks points to their slight oversaturation with Al_2O_3.

Table 2 shows the contents of major, trace, and rare-earth (REE) elements in the rocks of the three formations. Their average values for the rocks of the series basaltic andesite (basaltic trachyandesite)–andesite (trachyandesite) are shown in Fig. 4*a*. The rocks of the three formations show similar patterns of incompatible elements, particularly well-pronounced negative Ta–Nb and Ti anomalies typical of IAB (Kelemen et al., 2003). However, the studied volcanics are generally richer in almost all incompatible elements than IAB. The basaltic andesites and andesites of the Ust'-Kara and Shilka Formations are more enriched in these elements than the similar rocks of the Urdyugan Formation. The latter are characterized by significantly lower relative contents of P and Ti and a less fractionated REE pattern (average $(La/Yb)_{ch}$ ~ 17). The rocks of the Ust'-Kara and Shilka Formations show similar $(La/Yb)_{ch}$ values (~28) and patterns of incompatible elements. At the same time, the Ust'-Kara volcanics have lower contents of Sr and Ti, which might be due to the melt fractionation into plagioclase and titanomagnetite.

DISCUSSION

Magmatic evolution of the Ust'-Kara basin. Three phases of late Mesozoic magmatism have been established in the basin structure, which correspond to three volcanic units. The time gap between them is close to the error of
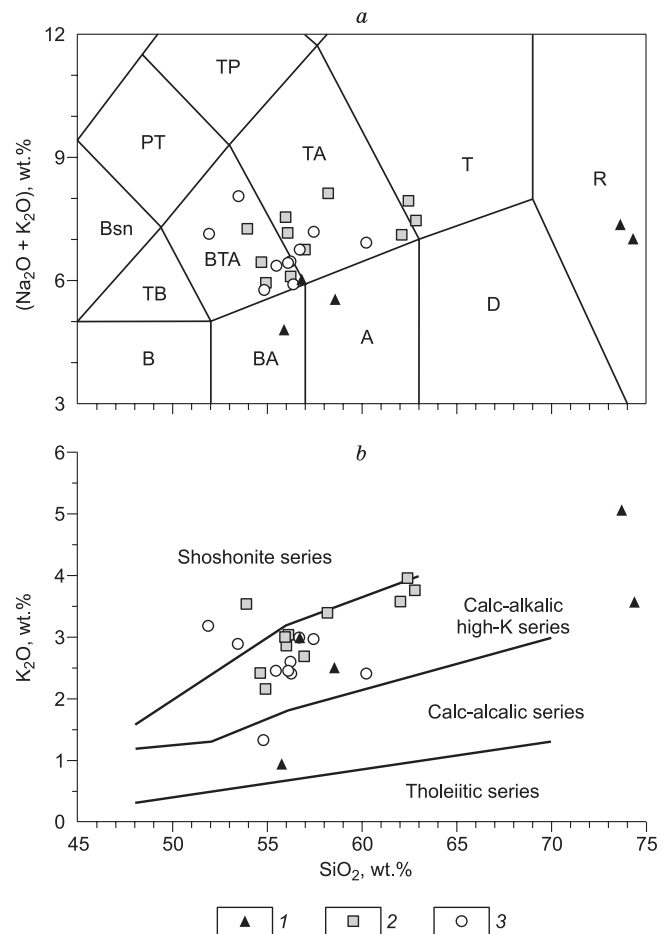
Fig. 3. $(Na_2O + K_2O)$–SiO_2 (Le Bas et al., 1986) (*a*) and K_2O–SiO_2 (Peccerillo and Taylor, 1976) (*b*) diagrams for the volcanics of the Ust'-Kara basin and the Kura River graben, constructed from the data in Table 2 and the results of chemical analyses. *1–3*, compositions of rocks of formations: *1*, Urdyugan, *2*, Ust'-Kara, *3*, Shilka. Rocks: B, basalt; BA, basaltic andesite; A, andesite; D, dacite; R, rhyolite; TB, trachybasalt; BTA, basaltic trachyandesite; TA, trachyandesite; T, trachyte; Bsn, basanite; PT, phonotephrite; TP, tephriphonolite.

volcanics dating. This gives grounds to consider the basin volcanism a single (although discrete) volcanic cycle, which began in the late Late Jurassic and ended in the first half of the Early Cretaceous. The products of volcanism of different stages differ from each other, especially the basaltic andesites and andesites of the Late Jurassic Urdyugan Formation, characterized by relatively high MgO (>5 wt.%) and low TiO_2 (<1 wt.%) contents. Similar magnesian andesites are known in many Middle–Late Jurassic volcanic structures of the Argun block (Pervov and Kononova, 1986), and all of them formed at the beginning of the particular stages of volcanic eruptions. For example, such magnesian volcanics are present in the Middle–Late Jurassic Shadoron and Unda–Daya Groups of the Shadoron basin (Kovalenko et al., 2015; Stupak et al., 2016). Andesites of these groups have high contents of MgO (up to 7.4 and 8.4 wt.%, respectively) and low contents of TiO_2 (0.9 and 0.8 wt.%). The somewhat

Table 2. Representative analyses of the chemical composition (wt.%) and trace-element and REE compositions (ppm) of rocks of the Ust'-Kara basin

Component	Shilka Formation							Ust'-Kara Formation								Urdyugan Formation		
	99-5*	99-7*	99-10*	99-29	99-2*	99-3*	99-4*	99-35	99-36	4-97	22-97	99-33	99-41	3-97	2-97	99-16	99-22	99-25
	BTA	BTA	BTA	BTA	TA	TA	TA	BTA	BTA	BTA	TA	TA	TA	TA	T	A	R	R
SiO_2	53.88	53.98	51.69	54.54	57.86	54.94	55.41	52.79	52.91	50.85	55.13	54.81	54.91	60.05	61.50	57.33	72.12	72.83
TiO_2	1.99	1.64	1.73	1.71	1.87	1.90	2.03	1.70	1.64	1.50	1.57	1.61	1.62	1.01	1.36	0.98	0.47	0.52
Al_2O_3	15.62	15.50	16.71	16.07	15.42	15.51	15.71	16.90	16.43	15.67	15.84	16.67	16.57	15.61	16.64	14.64	14.02	14.06
Fe_2O_3	8.42	8.91	10.13	8.19	7.95	7.52	8.80	7.96	7.71	8.72	6.99	7.99	7.63	4.76	6.35	7.14	2.33	1.72
MnO	0.12	0.22	0.17	0.10	0.05	0.12	0.08	0.08	0.11	0.10	0.10	0.08	0.06	0.08	0.08	0.12	0.03	0.01
MgO	2.20	3.55	2.15	4.03	2.35	2.22	2.65	2.82	3.08	3.54	2.28	3.14	3.43	2.23	0.87	5.91	0.77	0.51
CaO	6.74	8.26	5.57	6.67	3.04	7.23	3.85	7.49	8.13	6.50	4.62	5.63	5.01	5.81	3.42	6.12	0.79	1.31
Na_2O	3.40	4.39	5.02	3.85	4.35	3.66	4.10	3.90	3.66	3.52	4.48	4.45	3.93	3.44	3.93	3.00	2.27	3.37
K_2O	2.31	1.32	2.80	2.42	2.33	2.90	2.86	2.33	2.07	3.33	3.22	2.94	2.58	3.46	3.90	2.47	4.97	3.53
P_2O_5	1.02	0.74	0.75	0.78	0.92	0.94	1.01	0.58	0.57	0.55	0.54	0.60	0.61	0.35	0.48	0.26	0.15	0.16
LOI	4.40	1.60	3.35	1.69	3.85	3.04	3.55	3.53	3.70	5.55	5.26	2.11	3.63	3.24	1.43	2.17	2.13	2.04
Total	100.10	100.12	100.06	100.06	99.99	99.97	100.04	100.08	100.01	99.83	100.02	100.05	100.00	100.03	99.97	100.13	100.05	100.06
V	162	182	171	173	149	168	163	162	170	162	121	180	166	85	115	161	26	30
Cr	50	61	54	67	47	48	51	70	74	182	76	78	68	78	63	318	31	69
Co	25.8	26.2	32.4	24.4	19.8	20.3	24.2	20.6	24.1	34.7	15.4	22.1	22.6	13.8	14.8	29.9	4.69	3.28
Ni	25	30	45	25	22	22	24	26	29	63	27	27	24	28	27	96	13	14
Zn	132	123	116	134	137	125	135	120	114	124	113	118	117	91	100	85	73	30
Rb	54.1	31.2	69.5	72.0	52.5	76.1	61.6	50.4	28.5	80.4	85.0	86.5	58.4	132.0	170.0	74.0	131.0	121.0
Sr	942	879	1400	917	655	958	741	1000	1180	1220	629	1000	860	964	660	517	198	344
Y	24.6	26.4	26.0	21.4	24.0	24.1	23.1	15.3	16.4	22.3	17.8	18.8	14.6	14.5	15.3	21.2	8.94	9.21
Zr	459	396	317	303	440	450	451	233	243	285	308	295	266	266	345	210	158	204
Nb	27.4	25.0	20.2	19.9	25.5	26.3	26.5	13.6	14.9	20.4	19.9	16.7	15.3	16.0	20.8	11.7	10.5	12.1
Ba	1240	649	1330	898	1040	1070	1470	879	944	1480	927	1100	964	962	981	664	977	810
La	82.8	61.6	56.1	54.9	81.3	81.1	79.5	43.1	45.3	64.2	55.9	53.1	45.9	58.5	70.3	37.4	37.7	45.1
Ce	180.0	135.0	115.0	117.0	174.0	175.0	174.0	91.1	95.2	131.0	117.0	107.0	99.9	113.0	140.0	78.3	70.2	80.6
Pr	20.9	15.9	14.0	14.3	20.5	20.2	19.8	11.0	11.5	15.1	13.6	12.9	11.2	12.2	15.2	9.05	7.66	8.73
Nd	83.6	67.2	57.2	57.7	79.0	79.8	78.5	43.4	46.1	56.5	50.5	50.7	46.0	43.7	53.1	34.8	26.8	30.6
Sm	15.50	12.60	10.80	11.20	13.30	14.20	14.00	7.62	9.09	10.60	10.40	9.08	8.93	8.91	10.60	6.45	4.40	5.07
Eu	3.19	2.62	2.54	2.52	3.14	3.06	3.21	1.88	2.07	2.44	2.18	2.36	2.18	1.65	1.82	1.63	1.06	1.08
Gd	10.80	9.59	8.67	7.40	10.30	10.30	9.86	5.74	5.96	7.29	6.42	6.46	6.01	5.26	5.85	5.46	3.06	3.47
Tb	1.24	1.28	1.21	1.07	1.35	1.27	1.26	0.75	0.82	1.05	0.90	0.88	0.79	0.70	0.77	0.80	0.41	0.49
Dy	5.47	5.65	5.37	4.72	5.24	5.64	5.37	3.23	3.71	4.61	3.72	3.81	3.40	3.13	3.35	3.92	1.96	2.20
Ho	0.78	0.96	0.81	0.73	0.85	0.84	0.81	0.55	0.57	0.78	0.60	0.59	0.46	0.45	0.55	0.70	0.32	0.35
Er	2.19	2.69	2.42	1.95	2.10	2.24	2.16	1.41	1.62	2.11	1.64	1.63	1.30	1.15	1.35	2.15	0.70	0.85
Tm	0.31	0.35	0.31	0.22	0.27	0.29	0.31	0.17	0.21	0.28	0.20	0.21	0.19	0.18	0.18	0.29	0.11	0.10
Yb	1.50	1.98	1.92	1.52	1.51	1.86	1.64	1.15	1.25	1.61	1.13	1.25	1.20	1.01	1.00	1.81	0.73	0.62
Lu	0.27	0.31	0.27	0.23	0.23	0.24	0.25	0.16	0.16	0.27	0.19	0.19	0.15	0.15	0.16	0.30	0.09	0.10
Hf	10.20	9.27	6.99	7.56	9.83	10.60	9.65	5.28	6.53	6.78	7.07	7.11	6.58	6.53	7.83	6.10	4.38	5.63
Ta	1.44	1.16	0.95	1.04	1.35	1.31	1.51	0.77	0.82	1.17	1.18	0.92	0.83	0.91	1.25	0.80	0.70	0.82
Th	8.94	5.24	4.64	8.21	10.20	10.40	9.56	6.75	7.31	12.50	10.80	6.69	6.98	23.20	26.80	10.80	12.40	12.30
U	2.34	1.47	1.14	2.05	2.53	2.87	2.45	1.46	1.69	2.86	2.82	1.35	1.55	4.10	3.66	2.58	2.02	3.33

Note. The chemical composition was determined at the Institute of Geochemistry, Irkutsk, and the trace-element and REE contents, at the Institute of Precambrian Geology and Geochronology, St. Petersburg.
* Data from Stupak (2012). Rocks: BTA, basaltic trachyandesite; TA, trachyandesite; T, trachyte; R, rhyolite.

younger andesites of the Urdyugan graben are similar to them in some characteristics. Besides the above-mentioned petrochemical specifics, the andesites and basaltic andesites of the Urdyugan Formation have the same geochemical features as the andesites of the Shadoron Group (Fig. 4*b*), which indicates their formation under similar conditions.

The volcanics of the Ust'-Kara and Shilka Formations differ from the rocks of the Urdyugan Formation in higher total alkalinity, mainly because of higher contents of K_2O and TiO_2 and lower contents of MgO (Table 2). They also have higher contents of incompatible elements (Fig. 4*a*). The volcanics of the Ust'-Kara and Shilka Formation also differ despite their similar ages and petrochemical features. For example, the rocks of the Shilka Formation are enriched in almost all trace elements relative to the Ust'-Kara volcanics and, in addition, show different trends of their distribution relative to SiO_2 (Fig. 5).

The felsic volcanics of these formations are not related to mafic rocks by the accumulation trends of incompatible elements corresponding to fractionation processes (Fig. 5). They are depleted in trace elements. As shown for other late Mesozoic volcanic associations of the study region (Vorontsov et al., 2016; Stupak et al., 2018b), such features of felsic rocks permit them to be considered products of anatectic melting of crustal rocks under thermal effect of mafic melts.

The revealed difference in the composition of the same rocks of the three formations of the Ust'-Kara basin show that the content of MgO decreases and the contents of TiO_2, K_2O, P_2O_5, Zr, Nb, and REE increase in the course of the rock evolution (Fig. 5). At the same time, the geochemical spectra of these rocks are generally similar and typical of rocks of convergent settings.

Correlations and determination of the position of the Ust'-Kara basin in the system of late Mesozoic volcanic belts. As mentioned above, the Ust'-Kara basin formed in the northwest of the Argun terrane, at the intersection of the GX and EM volcanic belts, whose evolution was governed by different geodynamic processes.

The late Mesozoic structure of the study region is characterized by narrow grabens and basins controlling the distribution of Late Jurassic and Cretaceous continental deposits and volcanic units. Within the East Mongolian belt, grabens are mostly of NE orientation (~60º). Within the Argun terrane, grabens of N–NE orientation (~30º), including the Ust'-Kara one, are predominant. This difference, however, is insufficient to state the different nature of volcanism in the two areas.

Comparison of the volcanics of the Ust'-Kara basin with the coeval rocks of the EM and GX volcanic belts provides more significant information about the geodynamic mechanisms that controlled the late Mesozoic magmatic and tectonic activity in the northern part of the Argun terrane.

The Jixiangfeng, Shangkuli, and Yiliekede Formations of the GX volcanic belt are age analogues of the volcanic complexes of the Ust'-Kara basin. They accumulated within ~145–120 Ma and are made up of rocks of different compo-
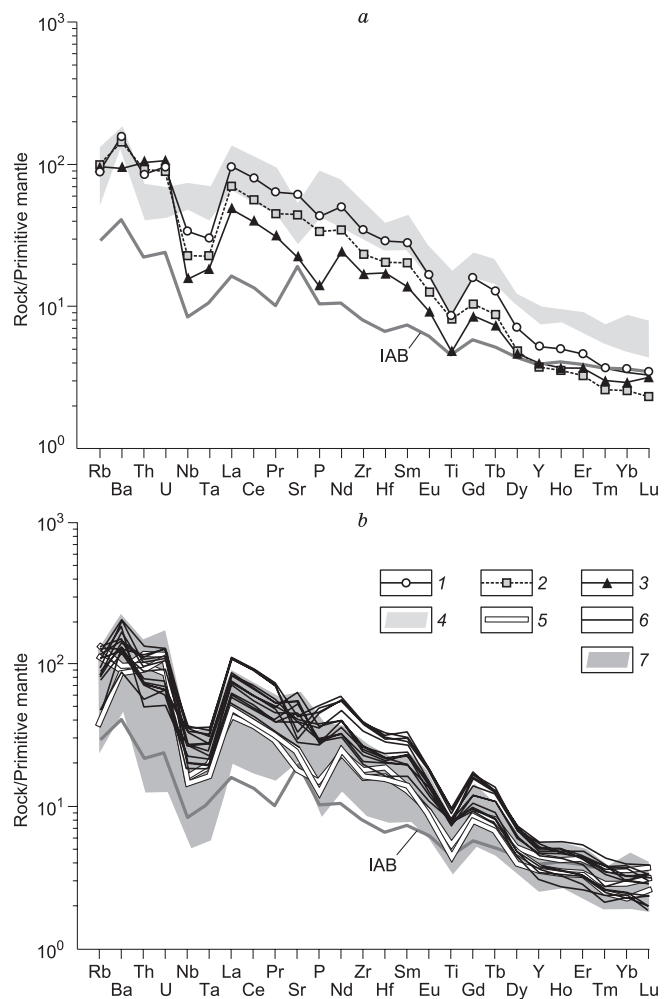
Fig. 4. Primitive-mantle-normalized (Sun and McDonough, 1989) trace-element and REE (ppm) patterns of the moderately mafic volcanics of the Ust'-Kara basin and Kuma River graben. *a*, Average compositions of the volcanics of the Shilka (*1*), Ust'-Kara (*2*), and Urdyugan (*3*) Formations in comparison with the rocks of the East Mongolian (EM) volcanic belt (*4*) (Dash et al., 2015; Stupak et al., 2018a); *b*, compositions of the rocks of the Urdyugan (*5*) and Ust'-Kara and Shilka (*6*) Formations in comparison with the rocks of the Great Xing'an volcanic belt and Shadoron basin (*7*) (Zhang et al., 2008b; Stupak et al., 2016). The average composition of continental IAB is given after Kelemen et al. (2003).

sitions, with a predominance of rhyolite and rhyodacite lavas and tuffs (Zhang et al., 2008b; Xu et al., 2013). In the Russian part of the belt, there are compositionally similar Late Jurassic–Early Cretaceous volcanic complexes of the Tulukui caldera (Shatkov et al., 2010) and Argun basins (Pavlova et al., 1990) (Fig. 6).

Within the EM belt, the Late Jurassic–Early Cretaceous stage of volcanism is confirmed by paleontological data (Frikh-Khar and Luchitskaya, 1978; Martinson, 1982), although the available geochronological dates are no older than 130 Ma (Dash et al., 2015; Stupak et al., 2018a). The Early Cretaceous volcanics are mostly trachybasalts and ba-
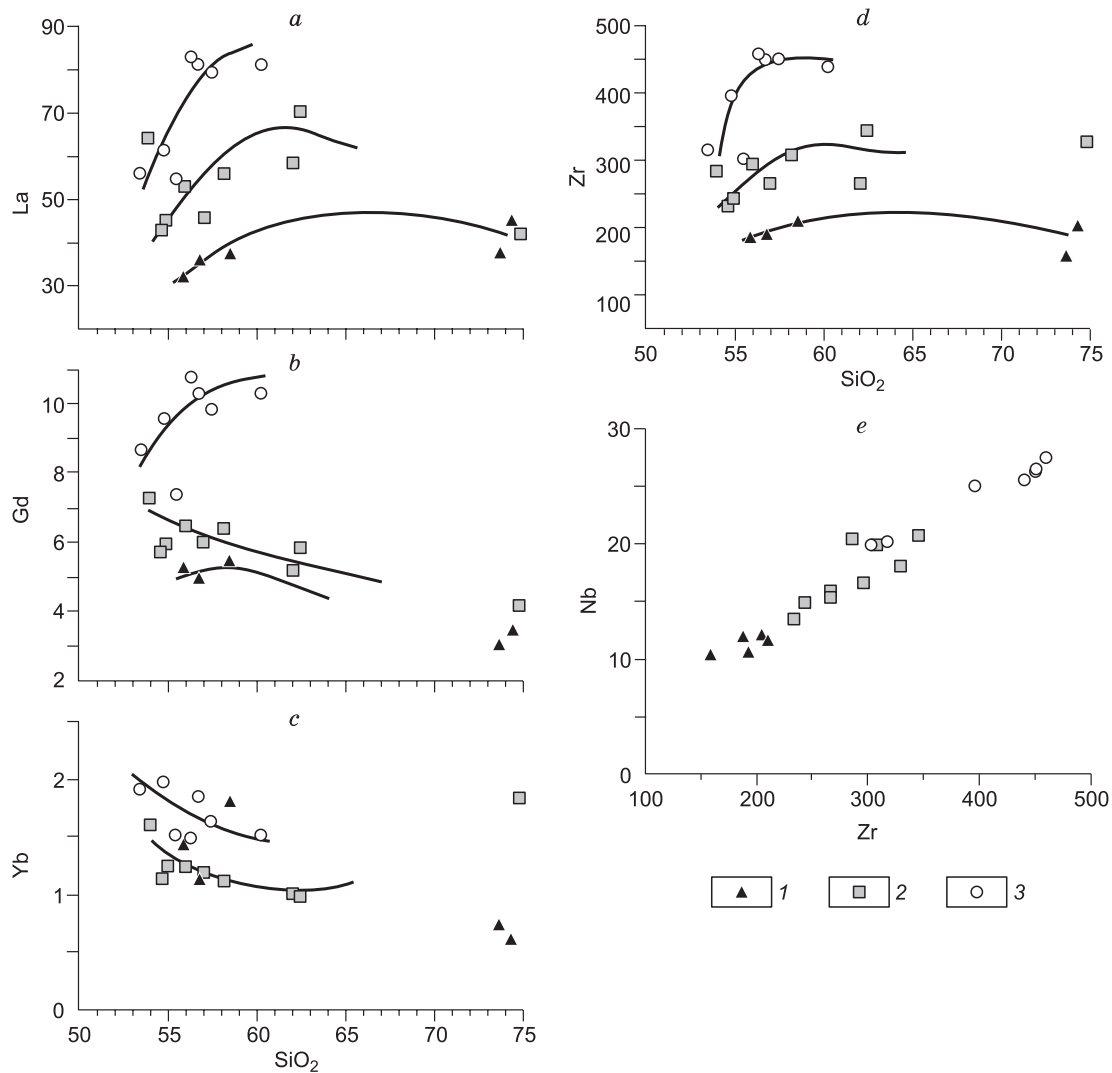
Fig. 5. Distribution of trace elements (ppm) relative to SiO_2 (wt.%) in the volcanics of the Ust'-Kara basin and Kuma River graben (from the data in Table 2). *1–3*, Compositions of rocks of formations: *1*, Urdyugan, *2*, Ust'-Kara, *3*, Shilka. Distribution trends of elements are shown.

saltic trachyandesites, whereas trachyandesites, trachydacites, and trachyrhyolites are subordinate.

The rocks of both the GX and EM belts differ in chemical composition. The lavas of the EM belt (Fig. 6, I) are richer in Ti and have high contents of total Fe and P and low contents of Mg. Mafic rocks (SiO_2 < 54 wt.%) prevail, whereas normal rocks are subordinate. In the GX belt, normal and felsic rocks are, on the contrary, predominant (Zhang et al., 2008b; Xu et al., 2013). In geochemical features the GX rocks are similar to convergent-margin rocks; they have the minimum contents of Ta, Nb, and Ti and show highly fractionated REE patterns, like IAB (Fig. 4b). The rocks of the EM belt differ from them in higher contents of almost all incompatible elements (Fig. 4a) and show less fractionated REE patterns. The relative contents of Ta and Nb in these rocks vary from a slight deficit to a small maximum ($(La/Nb)_n$ = 2.3–0.9). All this gives grounds to consider the

sources of magmatism in the study area to be similar to the intraplate sources of OIB (Stupak et al., 2018a).

The difference in the composition of igneous rock associations of the two belts is well seen in the diagrams of correlation between the ratios of incompatible elements, where the rocks of the GX and EM belts form separate composition fields with different trends of figurative points (Fig. 7). The EM rocks have rather low Zr/Nb ratios (<15) and more or less stable Nb/U, Ce/P, and Th/U ratios. They show a direct correlation of La/Yb, Th/Yb, and La/Nb with Zr/Nb. In the $(La/Nb)_n$–Zr/Nb diagram, the lower edge of this trend corresponds to the compositions $(La/Nb)_n \sim 1$, without a Nb deficit specific to rocks of convergent margins. The other edge of the trend is directed to the composition field of the GX rocks, which might indicate the participation of their sources (e.g., the metasomatized mantle of the mantle wedge) in the formation of the EM rocks. This participation
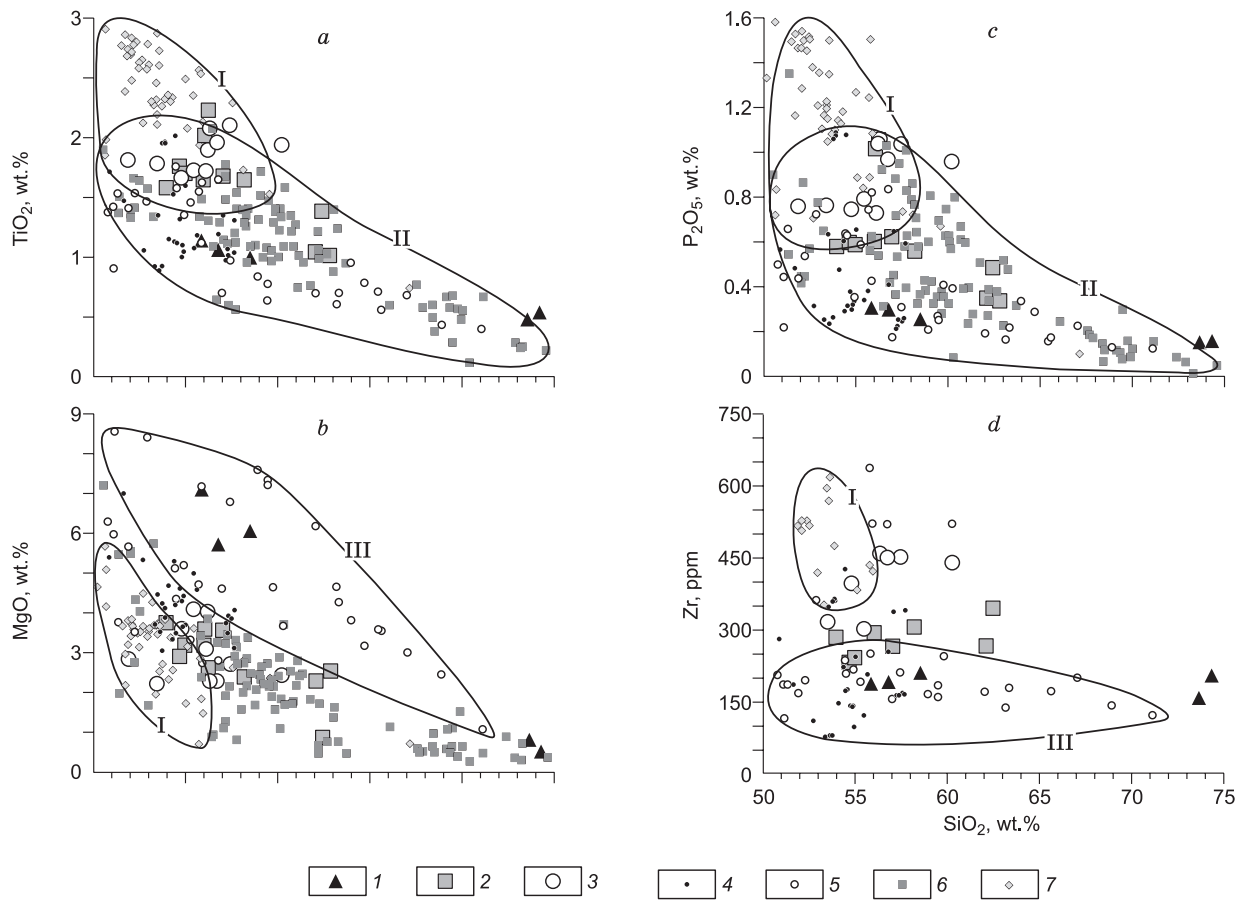
Fig. 6. Comparison of the compositions of the rocks of the Ust'-Kara basin and Kuma River graben and the compositions of the rocks of the East Mongolian and Great Xing'an volcanic belts. Rocks of: *1*, Urdyugan, *2*, Ust'-Kara, and *3*, Shilka Formations; *4*, northern part of the Great Xing'an belt (Zhang et al., 2008b); *5*, Shadoron basin (Kovalenko et al., 2015; Stupak et al., 2016); *6*, Argun basins (Pavlova et al., 1990); *7*, East Mongolian belt (Frikh-Khar and Luchitskaya, 1978; Dash et al., 2015; Stupak et al., 2018a). Composition fields of the rocks of: I, East Mongolian belt; II, Great Xing'an belt, including the rocks of the Argun basins; III, Shadoron basin.

might have determined a linear correlation between the ratios of incompatible elements. In contrast to the EM belt, the rocks of the GX belt show higher Zr/Nb ratios (>13) and wide variations in the contents of other indicator ratios of incompatible elements independent of Zr/Nb (Fig. 7).

Based on the above features of the EM and GX rocks, we can compare them with the Ust'-Kara basin rocks. In Fig. 4, the multielement patterns of the basin rocks are similar to those of the EM and GX mafic rocks. The basin rocks are similar to the GX rocks both in the shape of the multielement patterns and in the contents of elements (Fig. 4b). The difference between these rocks and the EM rocks are also well seen (Fig. 4a). The latter are characterized by higher contents of trace elements, especially HREE, a less pronounced Ta–Nb negative anomaly, and no fractionation of Th, U, Nb, and Ta.

Other discrimination diagrams also show similarity and difference of the above rocks. In Fig. 6, the Ust'-Kara basin rocks fall mostly in the composition field of the GX rocks. The volcanics of the Urdyugan Formation are most similar

in composition to the rocks of the Shadoron Group. Taking into account the Late Jurassic age of the Urdyugan Formation rocks, we assume that they belong to the Shadoron Group of the GX belt.

The similarity of the Ust'-Kara volcanics to the GX belt rocks is also well seen in the diagrams of correlation between the ratios of incompatible elements (Fig. 7). In the La/Yb, Th/Yb, La/Nb–Zr/Nb diagrams, the Ust'-Kara volcanics lie in the composition field of the GX belt but fall on the extension of the composition trends of the EM rocks. This suggests a certain genetic relationship between the Ust'-Kara volcanics and the EM rocks. In the Nb/U, Ce/Pb, Th/U–Zr/Nb diagrams, however, the Ust'-Kara rocks are clearly isolated from the EM rocks, which indicates different compositions of their sources.

Thus, the comparison shows a strong similarity between the rocks of the Ust'-Kara basin and the rocks of the GX volcanic belt at the Late Jurassic and Early Cretaceous stages of its evolution. This suggests that the convergent processes that determined the formation of the GX belt played
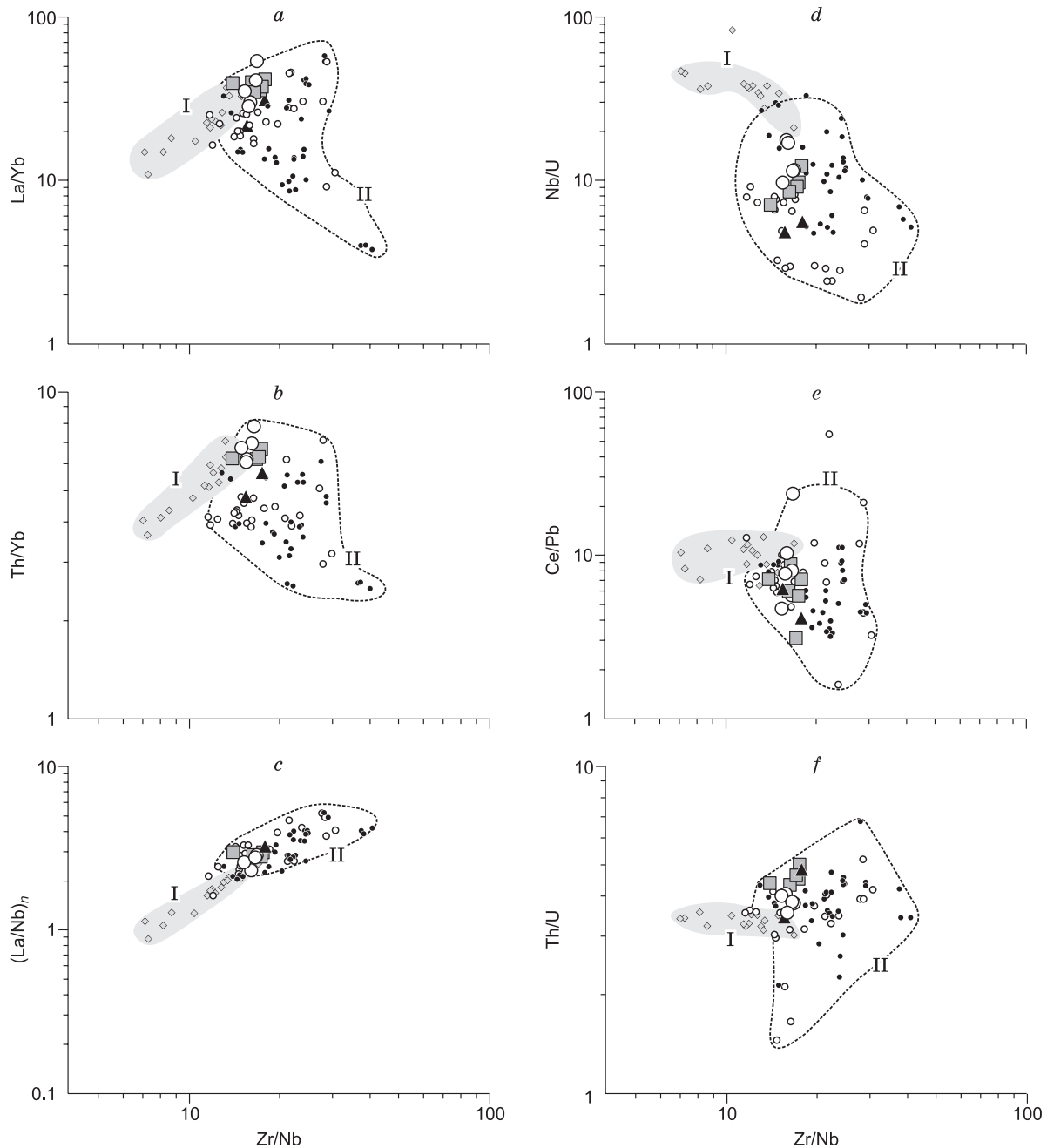
Fig. 7. Variations in the ratios of incompatible elements vs. Zr/Nb in the rocks of the Ust'-Kara basin and the East Mongolian and Great Xing'an volcanic belts. Constructed from the data in Table 2 and literature data (Zhang et al., 2008b, Dash et al., 2015, Stupak et al., 2018a). Designations follow Fig. 6.

a leading role in the late Mesozoic volcanism of the Argun terrane. We can also conclude that the mantle plume that controlled the formation of the EM belt affected negligibly the Early Cretaceous magmatism of the GX belt.

CONCLUSIONS

The late Mesozoic volcanism in the Ust'-Kara basin evolved in three stages: Tithonian–Berriasian (~150–143 Ma), Valanginian (~140–136 Ma), and Hauterivian (~134–

131 Ma). The evolution series includes primary normally al-kaline rocks (magnesian andesites) and younger predominant medium-alkali (basaltic trachyandesites–trachytes) and co-eval subordinate felsic rocks. The temporal evolution of melts was accompanied by an increase in the contents of incompatible elements in similar rocks.

In age and petrochemical and geochemical compositions the rocks of the Ust'-Kara basin are similar to the volcanics of the Great Xing'an belt and differ from the rocks of the East

Mongolian belt. This gives grounds to extend the Xing'an belt structures to the north, almost up to the Mongolo–Okhotsk suture, and thus to relate the late Mesozoic volcanism in the northwest of the Argun terrane to convergent processes that governed the formation of the Xing'an belt.

REFERENCES

Berzina, A.P., Berzina, A.N., Gimon, V.O., Krymskii, R.Sh., Larionov, A.N., Nikolaeva, I.V., Serov, P.A., 2013. The Shakhtama porphyry Mo ore-magmatic system (eastern Transbaikalia): age, sources, and genetic features. Russian Geology and Geophysics (Geologiya i Geofizika 54 (6), 587–605 (764–786).

Chernyshev, I.V., Lebedev, V.A., Arakelyants, M.M., 2006. K–Ar dating of Quaternary volcanics: methodology and interpretation of results. Petrology 14 (1), 62–80.

Dash, B., Yin, A., Jiang, N., Tseveendorj, B., Han, B., 2015. Petrology, structural setting, timing, and geochemistry of Cretaceous volcanic rocks in eastern Mongolia: Constraints on their tectonic origin. Gondwana Res. 27, 281–299.

Daukeev, S.Z., Kim, B.C., Li Tingdong, Petrov, O.V., Tomurtogoo, O. (Eds.), 2008. Atlas of Geological Maps of Central Asia and Adjacent Areas, 1:2,500,000. Geological Publishing House, Beijing.

Frikh-Khar, D.I., Luchitskaya, A.I., 1978. Late Mesozoic Volcanics and Associated Hypabyssal Intrusions of Mongolia [in Russian]. Nauka, Moscow.

Geologic Structure of the Chita Region. Explanatory Note to a Geological Map on a Scale of 1:500,000 [in Russian], 1997. Chita.

Kelemen, P.B., Hanghøj, K., Greene, A.R., 2003. One view of the geochemistry of subduction-related magmatic arcs, with an emphasis on primitive andesite and lower crust, in: Treatise on Geochemistry. Elsevier, Amsterdam, Vol. 3, pp. 593–659.

Kovalenko, D.V., Petrov, V.A., Poluektov, V.V., Ageeva, O.A., 2015. Geodynamic setting of Mesozoic mantle rocks of the Strel'tsov caldera (eastern Transbaikalia) and mantle domains of Central Asia and China. Vestnik KRAUNTs. Ser. Nauki o Zemle 28 (4), 24–39.

Le Bas, M.J., Le Maitre, R.W., Streckeisen, A., Zanettin, B., 1986. A chemical classification of volcanic rocks based on the total alkali–silica diagram. J. Petrol. 27 (3), 745–750.

Lebedev, V.A., Arakelyants, M.M., Gol'tsman, Yu.V., Oleinikova, T.I., 1999. Geochronology of magmatism, metasomatism, and ore formation processes in the Upper Urmi ore field (Khabarovsk Territory, Russia). Geologiya Rudnykh Mestorozhdenii 41 (1), 70–83.

Martinson, G.G. (Ed.), 1982. Mesozoic Lake Basins of Mongolia: Paleogeography, Lithology, Paleobiogeochemistry, Paleontology [in Russian]. Nauka, Leningrad.

Misnik, Yu.F., Kolodii, O.N., 1985. Late Mesozoic shift structure of the Shilka chain of the Mongolo–Okhotsk deep fault, in: Tectonics of Siberia [in Russian]. Nauka, Novosibirsk, Vol. 22, pp. 115–121.

Misnik, Yu.F., Shevchuk, V.V., 1975. The Shilka zone of the Mongolo–Okhotsk deep fault, in: Problems of Tectonics and Magmatism of Deep Faults [in Russian]. Vishcha Shkola, Lviv.

Pavlova, V.V., Trusova, E.K., Valenkov, S.B., 1990. Improvement of the Method of Division and Correlation of the Upper Mesozoic Reference Sections of Eastern Transbaikalia for Large-Scale Geological Survey [in Russian]. VSEGEI, Leningrad.

Peccerillo, A., Taylor, S.R., 1976. Geochemistry of Eocene calc-alkaline volcanic rocks from the Kastamonu area, Northern Turkey. Contrib. Mineral. Petrol. 58, 63–81.

Pervov, V.A., Kononova, V.A., 1986. Rock-forming minerals of magnesian andesites of the Shadoron depression (southeastern Transbaika-

lia) in the context of rock genesis problems, in: Rock-Forming Minerals of Igneous Rocks [in Russian]. Nauka, Moscow, pp. 126–138.

Pistsov, Yu.P., 1963. Tectonics of upper Mesozoic basins in eastern Transbaikalia. Geologiya i Geofizika 4 (9), 52–65.

Pistsov, Yu.P., 1982. Sedimentary formations of the Transbaikalian rift system. Sovetskaya Geologiya, No. 8, 59–69.

Shatkov, G.A., Berezhnaya, N.G., Lepekhina, E.N., Rodionov, N.V., Paderin, I.P., Sergeev, S.A., 2010. U–Pb (SIMS SHRIMP-II) age of volcanic rocks from the Tulukuev caldera (Streltsov uranium-ore cluster, eastern Transbaikalia). Dokl. Earth Sci. 432 (1), 587–592.

State Geological Map of the Russian Federation, Scale 1:1,000,000 (Third Generation). Aldan–Transbaikalia Series. Sheet N-50: Sretensk. Explanatory Note [in Russian], 2010. VSEGEI, St. Petersburg.

Steiger, R.H., Jager, E., 1977. Subcommission on Geochronology: convention on the use of decay constants in geo- and cosmochronology. Earth Planet. Sci. Lett. 36, 359–362.

Stupak, F.M., 2012. Hyaloclastites of southeastern Transbaikalia, in: Notes of the Transbaikalian Branch of the Russian Geographical Society [in Russian]. Izd. ZO RGO, Chita, pp. 118–130.

Stupak, F.M., Travin, A.V., 2004. The age of Late Mesozoic volcanogenic rocks of northern Transbaikalia (estimated by the $^{40}Ar/^{39}Ar$ method). Geologiya i Geofizika (Russian Geology and Geophysics) 45 (2), 280–284 (263–267).

Stupak, F.M., Kudryashova, E.A., Lebedev, V.A., 2016. On the Jurassic volcanism and on volcanoes in the Shadoron basin, Eastern Transbaikalia. J. Volcanol. Seismol. 10 (2), 86–99.

Stupak, F.M., Kudryashova, E.A., Lebedev, V.A., Gol'tsman, Yu.V., 2018a. The structure, composition, and conditions of generation for the Early Cretaceous Mongolia–East-Transbaikalia volcanic belt: the Durulgui–Torei area (southern Transbaikalia, Russia). J. Volcanol. Seismol. 12 (1), 34–46.

Stupak, F.M., Yarmolyuk, V.V., Kudryashova, E.A., Lebedev, V.A., 2018b. Early Cretaceous Kalakan magmatic area (Vitim region, northern Transbaikalia): stages of formation, magmatic sources, and tectonic setting. Russ. J. Pacific Geol. 12 (6), 539–548.

Sun, S.-s., McDonough, W.F., 1989. Chemical and isotopic systematics of oceanic basalts: implications for mantle composition and processes, in: Saunders, A.D., Norry, M.J. (Eds.), Magmatism in the Ocean Basins. Geol. Soc. London, Spec. Publ. 42, 313–345.

Voinovskii-Kriger, K.G., Lisovskii, A.L., 1927. The geologic structure of the area of the Ust'-Kara Village near the Shilka River (eastern Transbaikalia). Vestnik Geolkoma 2 (6), 1–5.

Vorontsov, A.A., Yarmolyuk, V.V., Komaritsyna, T.Yu., 2016. Late Mesozoic–Early Cenozoic rifting magmatism in the Uda sector of Western Transbaikalia. Russian Geology and Geophysics (Geologiya i Geofizika), 57 (5), 723–744 (920–946).

Wang, F., Zhou, X.-H., Zhang, L.-Ch., Ying, J.-F., Zhang, Yu-T., Wu, F.-Yu., Zhu, R.-X., 2006. Late Mesozoic volcanism in the Great Xing'an Range (NE China): timing and implications for the dynamic setting of NE Asia. Earth Planet. Sci. Lett. 251, 179–198.

Xu, W.-L., Pei, F.-P., Wang, F., Meng, E., Ji, W.-Q., Yang, D.-B., Wang, W., 2013. Spatial–temporal relationships of Mesozoic volcanic rocks in NE China: Constraints on tectonic overprinting and transformations between multiple tectonic regimes. J. Asian Earth Sci. 74, 167–193.

Yarmolyuk, V.V., Kovalenko, V.I., Ivanov, V.G., 1995. Late Mesozoic–Cenozoic intraplate volcanic province of Central and East Asia: a projection of the hot field of the mantle. Geotektonika, No. 5, 41–67.

Zhang, J.-H., Ge, W.-Ch., Wu, F.-Yu., Wilde, S.A., Yang, J.-H., Liu, X.-M., 2008a. Large-scale Early Cretaceous volcanic events in the northern Great Xing'an Range, Northeastern China. Lithos 102, 138–157.

Zhang, L.-Ch., Zhou, X.-H., Ying, J.-F., Wang, F., Guo, F., Wan, B., Chen, Z.-G., 2008b. Geochemistry and Sr–Nd–Pb–Hf isotopes of Early Cretaceous basalts from the Great Xinggan Range, NE China: Implications for their origin and mantle source characteristics. Chem. Geol. 256, 12–23.

Editorial responsibility: E.V. Sklyarov